J. Phys. Chem. Solids, 1974, Vol. 35, pp. 1683–1689. Pergamon Press. Printed in Great Britain

MAGNETIC AND CRYSTAL STRUCTURE OF COPPER(II) FLUORIDE

P. FISCHER and W. HÄLG

Delegation für Ausbildung und Hochschulforschung am Eidg. Institut für Reaktorforschung, 5303 Würenlingen, Switzerland

D. SCHWARZENBACH

Institut de Cristallographie de l'Université, Bâtiment des Sciences Physiques, Dorigny/Lausanne, Switzerland

and

H. GAMSJÄGER

Institut für anorganische, analytische und physikalische Chemie, Universität, Bern, Switzerland

(*Received* 4 *April* 1974)

Abstract—A powder sample of the monoclinic, weak ferromagnet CuF_2 was investigated by neutron diffraction. Using the profile method, the crystal structure was refined and the spin configuration determined. The layer type structure with planar quadratic fluorine coordination of Cu^{2+} ($3d^9$) and the magnetic structure are remarkably similar to those of AgF_2. The spin configuration is however different from the magnetic structures of other $3d$-fluorides; the magnetic unit cell is doubled with respect to the chemical cell ($a_m = 2a$, $P2_1/c$). The ordered magnetic saturation moment corresponds to quenched orbital momentum.

1. INTRODUCTION

Complementary to a former investigation of the weak $4d^9$ ferromagnet AgF_2[1], we performed the present neutron diffraction study of weakly ferromagnetic CuF_2[2], where Cu^{2+} has the $3d^9$ electron configuration. There seem to be striking analogies in the magnetic properties and the crystal structures of these compounds. On the other hand it is interesting to discuss the magnetic ordering of CuF_2 with respect to the well-known magnetism of the difluorides MF_2; M = Mn, Fe, Co, Ni[3], which possess the tetragonal rutile structure where the coordination of the divalent $3d$ metal ions by fluorine is almost regularly octahedral. Except for VF_2, which has a spiral spin structure[4], the antiferromagnetic fluorides MF_2 including CrF_2[5] (with a monoclinic distorted rutile structure isotypic to the structure reported for CuF_2) have a magnetic unit cell of the same size as the chemical unit cell. The magnetic moments of the metal ions at the unit cell corners are oriented antiparallel to the moment of the ion in the center of the unit cell (type 1 order).

Joenk and Bozorth[2] discussed the bulk magnetic properties of CuF_2, using this model. By measurements of the magnetic susceptibility, the Néel temperature T_N was determined to be 69 K. The basic antiferromagnetism of CuF_2 is further confirmed by the negative paramagnetic Curie temperature: $\theta = -200$ K. At temperatures below T_N, the existence of a weak ferromagnetic moment was established, which at 4·2 K corresponds to a canting angle for the spins of approximately only 0·01°.

The monoclinic crystal structure of CuF_2 was determined by Billy and Haendler[6], using single crystal X-ray diffraction techniques. Neutron diffraction allows a more accurate determination of the fluorine positions than X-ray diffraction, because the nuclear neutron scattering amplitudes of Cu and F are of comparable size. In particular, the knowledge of the fluorine coordination around copper is of physical interest with respect to super-exchange and crystal field effects. In view of the $3d^9$ electron configuration of octahedrally coordinated Cu^{2+}, strong Jahn–Teller distortions corresponding to the published structure are to be expected[7].

In the following we report, after a brief description of sample preparation and experimental procedures, on the refinement of the nuclear structure and on the determination of the magnetic

ordering of copper(II) fluoride. In particular, the results are discussed with respect to magnetic properties and crystal structures of related solids.

2. EXPERIMENTAL

Commercially available polycrystalline copper(II) fluoride (Koch–Light Laboratories, England) is light-blue colored and contains 56·28 at.% Cu, corresponding to less than 90 per cent CuF_2. It was purified by slowly heating finely powdered samples in a stream of dry hydrogen fluoride. Excessive heating periods and temperatures higher than 473 K should be avoided, since otherwise red products with a mole fraction of $F/Cu < 2$, presumably mixed valency compounds, will be formed. After cooling to room temperature under nitrogen, the material was transferred to a glove box filled with helium in order to prevent contact with the atmosphere. A white powder of the following composition was obtained (Found: Cu, 62·28; F, 37·5. Calc. for CuF_2: Cu, 62·58; F, 37·42%).

A sample was filled into a cylindrical vanadium container of 2 cm dia. and approx. 5 cm height which was then sealed vacuum-tight by electron welding. The neutron diffraction measurements were made on a triple-axis spectrometer (in the two-axis mode of operation) at reactor SAPHIR in Würenlingen. The wave-length $\lambda = (2{\cdot}347 \pm 0{\cdot}002)$ Å was obtained from a vertically bent graphite monochromator. A filter of pyrolythic graphite reduced higher order contaminations virtually completely. Apart from beam reductions, only one 20′–Soller collimator between sample and detector was used in the experiment.

3. REFINEMENT OF THE CRYSTAL STRUCTURE

Neutron diffraction patterns of CuF_2 were measured at 293, 77·3 and 4·2 K. The neutron diagram at 77·3 K in the paramagnetic state and at 4·2 K for the antiferromagnetically ordered phase are shown in Fig. 1.

At room temperature and 77·3 K, only nuclear reflections are present, which confirm the structure determined by Billy and Haendler [6]. CuF_2 crystallizes with the monoclinic space group symmetry $P2_1/c(C_{2h}^5)$. Fluorine occupies the general positions $4e$: $\pm(x,y,z;\ x,1/2-y,1/2+z)$, copper the special positions $2a$: (0,0,0; 0,1/2,1/2). Thus copper defines an "A sublattice" with respect to this unit cell. The published structure was described in the $P2_1/n$ setting, with copper forming an "I sublattice", as is indicated in Fig. 2. It appears then to be a considerably distorted rutile structure. For the present work, however, we prefer the $P2_1/c$ setting, because in this way the simplest description as a layer type structure and the smallest magnetic unit cell are obtained.

The measured neutron intensities were corrected for absorption; the product of the sample radius and the linear absorption coefficient $\mu R = 0{\cdot}31$ was determined by transmission measurements. The data analysis was made by means of Rietveld's profile refinement method [8]. As is evident from Fig. 1, the assumption of a Gaussian shape of the Bragg reflections is well fulfilled. The half-width HW of the peaks can be described by three resolution parameters according to the relation $HW^2 = PH \cdot tg^2\theta + QH \cdot tg\theta + RH$, where θ represents the Bragg angle. The nuclear scattering lengths used were published by Bacon [10].

The resulting structure parameters are summarized in Table 1, together with the values from the published X-ray diffraction experiments. The following instrumental parameters were refined but are not listed: scale factor C, zeropoint $2\theta_0$ of the scattering angles and the halfwidth parameters ($PH = 6{\cdot}5$, $QH = -3{\cdot}6$, $RH = 1{\cdot}0$, in units of (degrees)^2). Interatomic distances and angles of interest with respect to the octahedral fluorine coordination of copper and to probable superexchange interactions are summarized in Table 2.

The fluorine coordination of Cu^{2+} at the temperature of liquid helium is shown in Fig. 3. It may be described by a strongly distorted octahedron with point symmetry $\bar{1}$. There are four characteristic short bonds with approximate length 1·93 Å along the half-diagonals of an almost perfect CuF_4 square. Two long bonds of 2·298 Å which are not parallel to the normal of the square, form an angle of almost 90° with the shortest bond (1·917 Å) and the angle F4-Cu-F5 of 78·08° with the second CuF distance (1·932 Å). As shown in Table 2, the fluorine coordination of Cr^{2+} in CrF_2 is remarkably similar. On the other hand, the tetragonal fluorides with rutile structure show almost regular octahedral coordination with distances metal to fluorine of 2·0 to 2·1 Å. Compared to orthorhombic AgF_2 [1] the CuF_4 square is slightly less distorted than the AgF_4 square and the difference between long and short bonds is smaller.

Similar to AgF_2, the CuF_2 structure may be considered as being built of chessboard-like puckered layers of CuF_4 squares shown in Figs. 2 and 4. These layers are parallel to the (100) plane, and the complete structure is arrived at by stacking them along the a-axis. On the other hand, in AgF_2

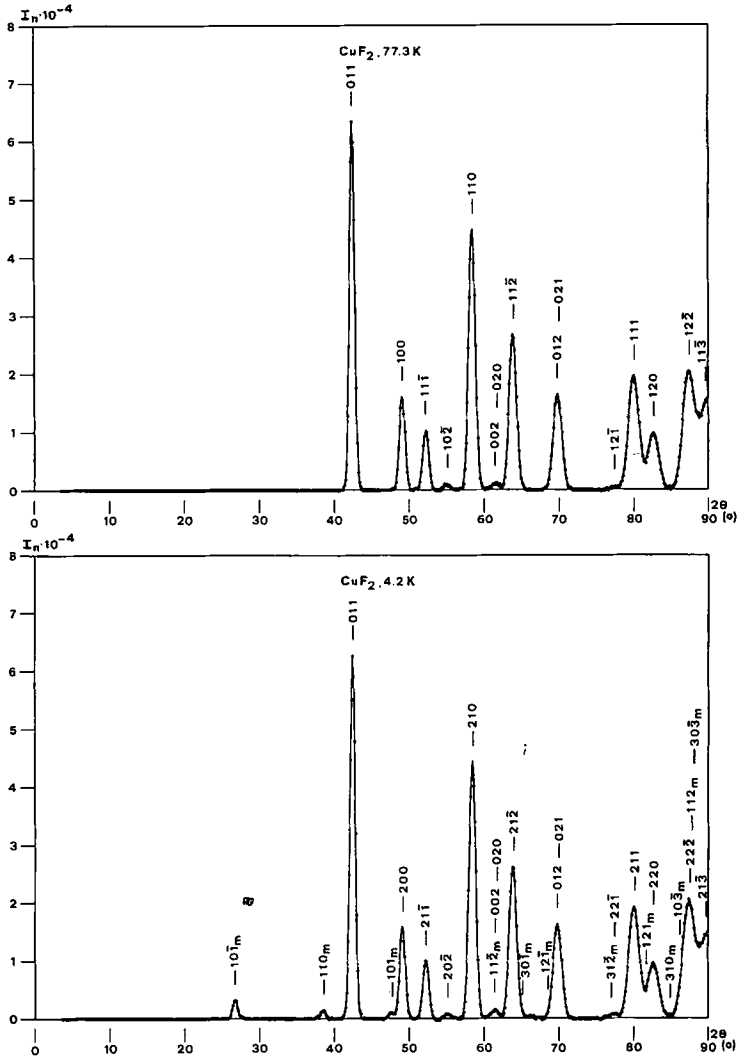

Fig. 1. Observed (points) and calculated (lines) absorption corrected neutron diffraction patterns of polycrystalline CuF_2 in the paramagnetic phase at 77·3 K and in the antiferromagnetically ordered state at 4·2 K (background subtracted). I_n = neutron intensity, 2θ = scattering angle. The upper diagram is indexed on the basis of the chemical unit cell in the $P2_1/c$ setting, whereas the lower diagram refers to the magnetic unit cell with P_a2_1/c symmetry. The index m designates magnetic Bragg peaks.

neighbouring square layers are related by a glide plane.

The contraction of the unit cell of CuF_2 with decreasing temperature is strongly anisotropic. The main change is in the distance $a \times \sin \beta$ (2·818 Å at 4·2 K) between the square layers which decreases in the temperature range from 293 to 4·2 K by 5·3‰, whereas b and c, i.e. the distances within the square layers, change only by 0·2–0·7‰. This implies an elongation with increasing temperature of the coordination octahedron of copper along the long bonds.

The crystal structure suggests mainly a 132° superexchange interaction Cu^{2+}—F^-—Cu^{2+} within a square layer involving two short Cu—F bonds with a direct distance Cu—Cu of 3·521 Å, and a 102° super-exchange interaction between two neighbouring layers via one long and one short Cu—F bond in CuF_6 octahedra sharing a common edge, with a direct Cu—Cu distance of $a = 3{\cdot}294$ Å.

4. DETERMINATION OF THE ANTIFERROMAGNETIC STRUCTURE

The 4·2 K neutron diffraction pattern of CuF_2 shown in Fig. 1 contains, in addition to the nuclear reflections, Bragg peaks due to three-dimensional

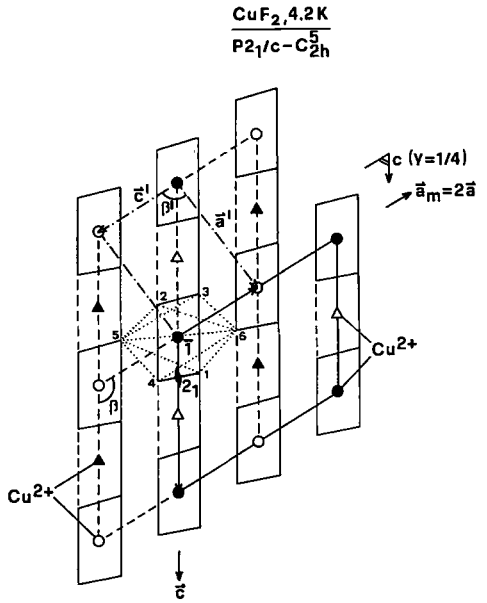

Fig. 2. Projection of the crystal and magnetic structure of CuF_2 (4·2 K) on the (c,a)–plane. Both the unit cells for the $P2_1/c$ setting (c,a indicated by arrows, $c_m = c$, $a_m = 2a$ for the magnetic structure) and the unit cell for the $P2_1/n$ setting (c', a') are shown. Fluorine occupies the corners of the CuF_4 squares around copper ions shown by full and broken lines. Dotted lines indicate the octahedral F^- coordination of Cu^{2+} at the origin. ●, ○: $y = 0$; ▲, △: $y = 1/2$; filled (open) symbols indicate magnetic moments pointing "up" ("down").

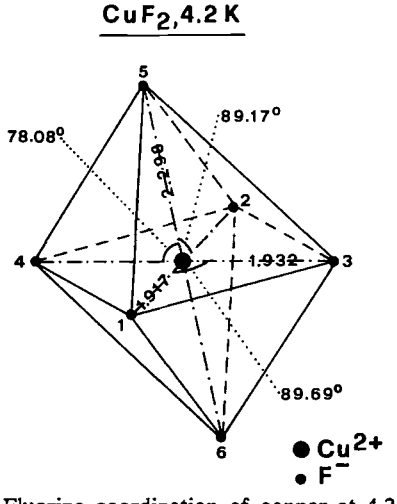

Fig. 3. Fluorine coordination of copper at 4·2 K. The distances are given in Å units.

antiferromagnetic long-range order. These magnetic reflections can be indexed on the basis of a magnetic unit cell, which is doubled along the a axis (setting $P2_1/c$) with respect to the chemical cell. Only the magnetic peaks $10\bar{1}_m$, 110_m and 101_m are clearly visible.

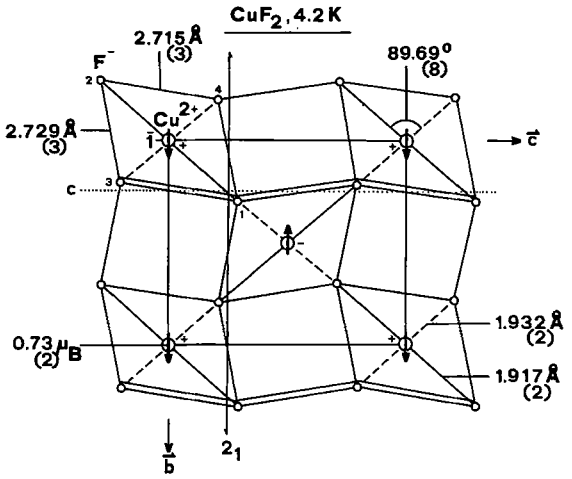

Fig. 4. Characteristic, puckered layers of CuF_4 squares in CuF_2 at 4·2 K. Double lines indicate positive x values.

The highest symmetric Shubnikov group related to $P2_1/c$ and containing an antitranslation (a)' is P_a2_1/c [12]. Table 3 shows the orientations of the magnetic moments (axial vectors) in this case. The x- and z-components have the same $+--+$ pattern, which leads to allowed magnetic reflections with Miller indices $h = 2u + 1$, $k + b = 2v + 1$; u,v = integers. This configuration suffices to explain the appearance of the observed magnetic peaks; the $+-+-$ pattern of the y-components leads to allowed but experimentally not observed reflections with $h = 2u + 1$, $k + b = 2v$. This might suggest zero or very small y-components. Magnetic contributions to nuclear reflections would arise from a ferromagnetic component whose existence is not possible under the symmetry P_a2_1/c.

Refinement of the model with the magnetic moment component $\mu_y = 0$, using the three observed magnetic peaks, resulted in $\mu_x = (0{\cdot}85 \pm 0{\cdot}03)\mu_B$, $\mu_z = (0{\cdot}37 \pm 0{\cdot}06)\mu_B$, $\mu = (0{\cdot}73 \pm 0{\cdot}03)\mu_B$ with $R_m = 20{\cdot}9$ per cent ($RW_p = 5{\cdot}1$ per cent). The calculations were based on a theoretical spherical neutron magnetic form factor of Cu^{2+} [13]. Using the general Halpern–Johnson formula for the magnetic neutron intensity [8], contributions from hkl and $h\bar{k}l$ reflections (having the same interplanar spacing d) were superimposed. By assuming however the $+--+$ arrangement also for the y-components of the magnetic moments, i.e. the Shubnikov group $P_s\bar{1}$ with the additional requirement of only parallel and antiparallel moments, the fit is already improved for the contrary case $\mu_x = \mu_z = 0$, resulting in $\mu_y = \mu = (0{\cdot}71 \pm 0{\cdot}02)\mu_B$ and $R_m = 10{\cdot}9$ per cent ($RW = 4{\cdot}9$ per cent). Since the profile intensities (RW_p) are

Table 1. Structure parameters of CuF_2, and for comparison those of CrF_2[5]

	CuF_2				CrF_2
	X[6] 293 K	*N* 293 K	*N* 77·3 K	*N* 4·2 K	*N*, *X* 298 K
a,a' [Å]	3·32, 4·59	3·309(3)	3·296(3)	3·294(3)	3·505, 4·732
b,b [Å]	4·54, 4·54	4·569(4)	4·568(4)	4·568(4)	4·718, 4·718
c,c' [Å]	5·34, 3·32	5·362(5)	5·360(5)	5·358(5)	5·560, 3·505
β,β' [°]	121·44, 96·67	121·11(3)	121·15(3)	121·17(3)	122·26, 96·52
x_F,x'_F	0·267, 0·300 0·256[9]	0·2558(6)	0·2556(5)	0·2556(6)	0·27, 0·30
y_F,y'_F	0·300, 0·300	0·2968(4)	0·2978(3)	0·2980(3)	0·30, 0·30
z_F,z'_F	0·300, 0·033 0·044[9]	0·2951(5)	0·2942(4)	0·2944(4)	0·30, 0·03
B_{Cu} [Å^2]		−0·09(8)	−0·15(7)	−0·11(6)	
B_F [Å^2]		0·21(9)	−0·06(8)	0·05(8)	
μ_x [μ_B]				0·26(9)	
μ_y [μ_B]				0·68(3)	
μ_z [μ_B]				0	
μ [μ_B]				0·73(2)	
R_n		0·017	0·017	0·015	
R_m				0·093	
RW_p		0·051	0·044	0·047	

N indicates results from neutron diffraction, *X* refers to X-ray investigations. The standard deviations, given in parentheses, relate to the last digit. Unprimed and primed lattice constants *a*, *b*, *c*, β, etc. refer to the $P2_1/c$ and $P2_1/n$ cells, respectively. x_F, y_F, z_F = position parameters of fluorine; *B* = Debye–Waller parameter (temperature factor $e^{-B(\sin\theta/\lambda)^2}$); μ_x, μ_y, μ_z = components of the magnetic moment along **a**,**b**,**c**; μ = magnitude of the total magnetic moment. R_n,R_m, and RW_p are the usual ratio criteria for agreement between calculated and observed intensities: R_n for nuclear, R_m for magnetic integrated, and RW_p for weighted profile intensities[8].

Table 2. Selected distances and angles in CuF_2 in comparison to those of CrF_2[5]

No.	Type	Atom Position	Distance (Å) / Angle (°)	CuF_2 Temperature (K) 293	77·3	4·2	CrF_2 298
0	Cu	0, 0, 0	0–1, 0–2*	1·917(2)	1·916(2)	1·917(2)	1·999
1	F	x_F, y_F, z_F	0–3, 0–4*	1·936(2)	1·934(2)	1·932(2)	2·036
2	F	$-x_F$, $-y_F$, $-z_F$	0–5, 0–6*	2·310(3)	2·300(2)	2·298(3)	2·374
3	F	x_F, $\frac{1}{2}-y_F$, $-\frac{1}{2}+z_F$	1–3, 2–4*	2·715(3)	2·715(3)	2·715(3)	2·820
4	F	$-x_F$, $-\frac{1}{2}+y_F$, $\frac{1}{2}-z_F$	1–4, 2–3*	2·734(3)	2·730(2)	2·729(3)	2·887
			0–7	3·522(2)	3·521(2)	3·521(2)	3·646
5	F	$-1+x_F$, $\frac{1}{2}-y_F$, $-\frac{1}{2}+z_F$	1–0–3, 2–0–4*	89·61(8)	89·69(7)	89·69(8)	88·66
6	F	$1-x_F$, $-\frac{1}{2}+y_F$, $\frac{1}{2}-z_F$	1–0–4, 2–0–3*	90·39(8)	90·31(7)	90·31(8)	91·34
7	Cu	$0,\frac{1}{2},\frac{1}{2}$	1–0–6, 2–0–5*	89·09(7)	89·12(6)	89·17(6)	88·78
8	Cu	1, 0, 0	1–0–5, 2–0–6*	90·91(7)	90·88(6)	90·83(6)	91·22
			3–0–6, 4–0–5*	78·0(1)	78·11(8)	78·08(8)	75·00
			3–0–5, 4–0–6,* 0–3–8, 0–6–8	102·0(1)	101·89(8)	101·92(8)	105·00
			0–1–7	132·2(1)	132·26(9)	132·3(1)	129·3

Estimated standard deviations are given in parentheses. * concerns the coordination around Cu(0, 0, 0).

obviously dominated by the strong nuclear reflections, we used for further calculations the measured integrated intensities of the three observed magnetic peaks, corrected for scale and Lorentz factors and divided by the multiplicity as obtained from the profile fit (for $\mu_x = \mu_z = 0$). Assuming a general moment orientation (+ − − + configuration) the calculated intensity (averaged over *hkl* and $h\bar{k}l$,

Table 3. Orientations of the magnetic moments with components μ_x, μ_y, and μ_z for the Shubnikov group P_a2_1/c and the special positions $2a(0, 0, 0)$

x	y	z	μ_x	μ_y	μ_z
0	0	0	+	+	+
1/2	0	0	−	−	−
0	1/2	1/2	−	+	−
1/2	1/2	1/2	+	−	+

which are not equivalent under the triclinic symmetry) is $I_m^{calc} = 16(0{\cdot}2695)^2\mu^2f^2e^{-2}\ {}^3\mathrm{Cu}^{(\sin/\lambda)^2}\{1 - (d/\mu)^2\,[(h\mu_x/a)^2 + (k\mu_y/b)^2 + (l\mu_z/c)^2 + 2hl\mu_x\mu_z/ac]\}$, where μ denotes the ordered magnetic moment in units of Bohr magnetons[8]. If the moment orientation is described in a Cartesian coordinate system with ξ parallel to the c axis, ζ parallel to the b axis and η perpendicular to the (ζ, ξ) plane and with ϑ and ρ being the polar angles to the ζ and ξ axes, then one obtains $\mu_x = \mu \sin\vartheta \sin\rho/\sin\beta$, $\mu_y = \mu\cos\vartheta$, $\mu_z = \mu \sin\vartheta (\cos\rho - \sin\rho \cot\beta)$. I_m^{calc} values were computed on a coarse grid in (ϑ, ρ) space and compared to I_m^{obs} in order to determine approximately best values for the angles ϑ and ρ and the magnetic moment. Some illustrative results are given in Table 4. Clearly the magnetic moments orient within the (a, b) plane, with the main component along the b axis. The relative signs of the x- and y-components cannot be determined from the present neutron results (as can be seen from the formula of I_m^{calc}). The first possible solution with positive μ_x and μ_y values was used for a final profile refinement including all magnetic and nuclear reflections in the scattering angle range of the measurement. The results are summarized in Table 1.

According to this model, the antiferromagnetic structure of CuF_2 consists of ferromagnetic planes parallel to (102) in the $P2_1/c$ setting, with antiparallel moment orientation in adjacent layers. Within the characteristic sheets formed by CuF_4 squares, copper atoms centered in squares with a common fluorine atom have opposite spin directions. Neighbouring layers show also antiparallel moment orientations. At 4·2 K, the magnetic moments of magnitude $(0{\cdot}73 \pm 0{\cdot}02)\mu_B$ are tilted $(21 \pm 6)°$ from the b axis in the (a, b) plane. The magnitude of the moment indicates quenching of the orbital contribution due to the strong crystalline electric field, i.e. it corresponds approximately to the spin only saturation value of Cu^{2+} with $3d^9$ electron configuration (the free ion ground state ^2D splits in the case of regular octahedral coordination into a $\Gamma_3 = E$ doublet and a $\Gamma_5 = T_2$ triplet, further reduction of the degeneracy for planar quadratic coordination). Corresponding to the observed weak ferromagnetism[2] a small ferromagnetic moment component perpendicular to the (a, b) plane is possible, but it cannot be detected by unpolarized neutrons. However, the "overall" symmetry of such a magnetic structure with ferromagnetic moment components would only correspond to the space group $P\bar{1}$, disregarding additional constraints.

Table 4. Possible magnetic moment orientations of CuF_2 at 4·2 K

RW	ϑ (°)	ρ (°)	μ	μ_x (μ_B)	μ_y (μ_B)	μ_z (μ_B)
0·264	90	90	0·74	0·86	0	0·45
0·131	0	0	0·70	0	0·70	0
0·025	30	120	0·75	0·38	0·65	0·01
0·025	30	300	0·75	−0·38	0·65	−0·01

$RW^2 = \sum_j [(I_m^{calc} - I_m^{obs})/\Delta I_m^{obs}]_j^2 \Big/ \sum_j (I_m^{obs}/\Delta I_m^{obs})_j^2$.
$I_{obs}^{101} = 0{\cdot}50 \pm 0{\cdot}01$, $I_{obs}^{110} = 0{\cdot}23 \pm 0{\cdot}01$, $I_{obs}^{101} = 0{\cdot}45 \pm 0{\cdot}03$.

5. CONCLUDING REMARKS

The magnetic structure of CuF_2 represents a new type of ordering in the group of the otherwise well-known fluorides MF_2 of the elements M belonging to the iron group. In the $P2_1/n$ setting, the magnetic unit cell of CuF_2 is doubled in the a′ and c′ directions with respect to the chemical cell, corresponding to the propagation vector $\pi(\mathbf{a}^{*\prime} + \mathbf{c}^{*\prime})$ in reciprocal space. In the orthorhombic structure of $CrCl_2$[5], a comparable type of magnetic structure was found, but with doubling along the b' and c' axes. Both cases correspond (in the description as distorted rutile structures) to a body-centered tetragonal, antiferromagnetic ordering of the third kind, which is known from molecular field theory of magnetically ordered states[14] (exchange constants $J_3 < 0$ for $CrCl_2$ and $J_2 < 0$, $|J_3| < |J_2|$ for CuF_2).

There is a close similarity in the magnetic structures of CuF_2 and AgF_2, presumably caused by comparable super-exchange interactions and similar electronic configurations in these related layer type structures. In both cases, the metal ions M in corner-linked MF_4 squares have opposite moment directions, and neighbouring layers have antiparallel spin orientations. The ordered magnetic moments are oriented predominantly parallel to the characteristic layers.

Depending on the magnitudes of the different

exchange interactions, there might exist in CuF_2 a temperature region, where two-dimensional magnetic correlations corresponding to the layer type structure dominate. However, because of the small magnetic moment of copper(II), it is difficult to obtain direct diffraction evidence for such a phenomenon from studies by means of unpolarized neutrons.

The measured ordered antiferromagnetic moment of Cu^{2+}: $(0{\cdot}73 \pm 0{\cdot}02)\mu_B$ at 4·2 K is smaller than the spin only value of $2S\mu_B = 1\mu_B$. One expects at this temperature ($T_N = 69$ K) almost complete saturation of the magnetic moment (the ferromagnetic component is known to be very small). The moment reduction might be caused to some extent by imperfections, e.g. impurities, but is more probably due to quantum spin wave[15] and covalency[16] effects.

Acknowledgements—We are indebted to Dr. P. Baertschi, head of the chemistry department of EIR, with respect to sample preparation. Moreover, we wish to thank our colleagues of the neutron scattering group, Mr. M. Koch, Mr. A. Erdin and Mrs. V. Stämpfli of delegation AF, as well as the staff of reactor SAPHIR for support of this investigation. The computer centers of EIR and ETH provided the calculation time. Finally it is a pleasure to thank Dr. B. O. Loopstra, Reactor Centrum Petten, The Netherlands, for initial powder neutron diffraction measurements.

REFERENCES

1. Fischer P., Roult G. and Schwarzenbach D., *J. Phys. Chem. Solids* **32**, 1641 (1971); Fischer P., Schwarzenbach D. and Rietveld H. M., *J. Phys. Chem. Solids* **32**, 543 (1971).
2. Joenk R. J. and Bozorth R. M., *J. appl. Phys.* **36**, 1167 (1965).
3. Erikson R. A., *Phys. Rev.* **90**, 779 (1953).
4. Lau H. Y., Stout J. W., Koehler W. C. and Child H. R., *J. appl. Phys.* **40**, 1136 (1969).
5. Cable J. W., Wilkinson M. K. and Wollan E. O., *Phys. Rev.* **118**, 950 (1960).
6. Billy C. and Haendler H. M., *J. Am. Chem. Soc.* **79**, 1049 (1957).
7. Goodenough J. B., In: *Magnetism and the Chemical Bond*, p. 242. Interscience, Wiley, New York (1963).
8. von Wartburg W., *Report* AF-SSP-46, Würenlingen (1970); Rietveld H. M., *RCN Report* 104, Petten, The Netherlands (1969).
9. Wyckoff R. W. G., *Crystal Structures*, Vol. 1, p. 264. Interscience, Wiley, New York (1963).
10. Bacon G. E., *Acta Crystallogr.* **A28**, 357 (1972).
11. Busing W. H., Martin K. O. and Levy H. A., ORNL-TM-**306**, Oak Ridge National Laboratory, U.S.A. (1962).
12. Opechowski W. and Guccione R., *Magnetism* **2A**, p. 105, Academic Press, New York (1965).
13. Menzinger F., Cox D. E., Frazer B. C. and Umebayashi H., *Phys. Rev.* **181**, 936 (1969).
14. Smart J. S., *Effective Field Theories of Magnetism*, p. 105, W. B. Saunders Company, London (1966).
15. Keffer F., *Handbuch der Physik* **18/2** (Editor S. Flügge), p. 115, Springer, Berlin (1966).
16. Hubbard J. and Marshall W., *Proc. Phys. Soc.* **86**, 561 (1965).